Technical Report #25

Adsorption of H$_2$ Isotopes on ZnO: Coverage Induced

IR Frequency Shifts and Adsorbate Geometry

Gregory L. Griffin and John T. Yates, Jr.

Surface Science Division
National Bureau of Standards
Washington, DC   20234

February, 1982

82 02 22 007

Adsorption of H_2 Isotopes on ZnO: Coverage Induced
IR Frequency Shifts and Adsorbate Geometry

Gregory L. Griffin* and John T. Yates, Jr. **

Surface Science Division
National Bureau of Standards
Washington, D. C. 20234

*NRC Postdoctoral Research Associate, 1979-80
Permanent address: Department of Chemical Engineering and Materials Science
                     University of Minnesota, Minneapolis, MN 55455

** Address after March 1, 1982: Department of Chemistry
                                 University of Pittsburgh
   Pittsburgh, Pennsylvania 15260

Abstract

The coverage dependence of the IR stretching frequencies for dissociative Type I adsorption of H_2 and D_2 on ZnO powders has been measured using transmission IR spectroscopy. By comparing the frequency shifts observed when the isotopic composition of the adsorbate is varied at constant total coverage with the shifts observed when the total coverage of either pure component is varied, we can separate the dynamic and static contributions to the coverage induced frequency shifts. The ZnH and ZnD shifts are due primarily to electrodynamic interactions. The observed shifts are in good agreement with the Hammaker model for dynamic dipole-dipole interactions, if adsorption is assumed to occur on (2 x 2) reconstructed ZnO (0001) surface planes. In contrast, the OH and OD shifts are due to electrostatic and inductive interactions. The electrostatic contribution can be estimated using a modification of Buckingham's treatment of local environment effects. A qualitative model, based on electron localization effects, is presented to explain the observed inductive contribution.

I. Introduction

The adsorption of H_2 on ZnO has received renewed attention in recent years because ZnO is a primary component in commercial methanol synthesis catalysts (1). Klier (2) has suggested that the role of the ZnO component in these catalysts is to provide sites for the dissociative adsorption of H_2, since H_2 is known to adsorb dissociatively on pure ZnO (3-5). The active sites for this so-called Type I adsorption of H_2 on pure ZnO consist of pairs of Zn and O surface atoms:

$$H_2 + -Zn - O - \longrightarrow \quad \begin{matrix} H & H \\ | & | \\ -Zn - & O - \\ | & | \end{matrix} \tag{1}$$
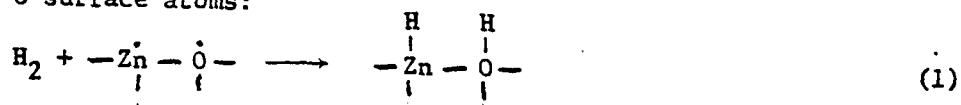
However, little additional information is available about the geometry of Type I adsorption sites on ZnO.

One method for obtaining information about the geometry of adsorbed species is to measure their vibrational frequency shifts as a function of adsorbate coverage (6). These frequency shifts contain information about both the separation and the relative orientation of adsorbed species. By varying both the total coverage and the isotopic composition of the adsorbate, it is possible to separate the dynamic dipole contribution to the frequency shift from the contribution due to static dipole or chemically-induced interactions (7).

Previous workers have reported that the coverage-induced ZnH and OH frequency shifts on ZnO were independent of isotopic composition (8). However, while performing experiments for our previously reported study of the energetics of Type I H_2 adsorption (5), we observed that the isotopic frequency shift behavior was somewhat more complex. Moreover, a quantitative discussion of the cause of the frequency shifts for Type I adsorption has not been given. Therefore, the present investigation was undertaken.

In this paper we report the coverage-induced frequency shifts for pure

(handwritten margin note: "ω = function of coverage")

H_2 and pure D_2 adsorbed on ZnO, and for H_2:D_2 adsorbate layers as a function

of composition. By comparing the pure- and mixed- isotope results, we show

that the ZnH shift is primarily caused by dynamic dipole interactions, while

the OH shift is mainly due to static interactions. Possible geometries for

the Type I adsorption sites are discussed, and evidence is given supporting

the partially reconstructed ZnO (0001) surface. Using this geometry, we show

that the observed ZnH shift is described quite well by Hammaker's model for

dynamic dipole interactions (10). We also discuss possible causes for the

observed OH shift, and conclude that the static shift contains two contri-

butions with opposite signs: An electrostatic effect that can be described

by Buckingham's treatment of local environment effects (11), and an inductive

effect caused by electron localization at neighboring adsorption sites, which

produces a change in the reference adsorbate bond polarity.

II. Experimental

The IR sample cell and ion-pumped gas handling system used in this work

were described previously (5). The ZnO samples (Kadox-25 , New Jersey Zinc

Co.) were prepared as pressed disks, evacuated to 673 K, and cooled in O_2 to

improve IR transmission. Adsorbate gases (H_2, HD, and D_2; Matheson) were

used as received.

(handwritten margin note: "NJ Disclaimer")

Absolute intensity measurements for all four species (OH, OD, ZnH, ZnD)

as a function of coverage were obtained by recording IR spectra of known

amounts of H_2 or D_2 adsorbed on a sample. The amount of each gas adsorbed

was determined by measuring the area under its temperature programmed desorp-

tion curve (5). The integrated IR intensities were evaluated approximately

as the product of the height of the absorbance peak times the full width at

half maximum. We estimate the accuracy of specific absorbance values deter-

mined in this way to be $\pm$ 10%.

Infrared frequency shifts in the pure adsorbate experiments were measured at 300 K by varying the pressure of H_2 or D_2 in the cell from zero to 100 torr. Adsorbate coverages in these experiments were determined from the IR intensities. For the mixed isotope experiments, the sample was exposed to $H_2:D_2$ mixtures of various compositions at a constant total pressure of 88 torr, in order to maintain saturation coverage of the Type I sites.

III. Results

Survey spectra of pure H_2 and pure D_2 adsorbed separately on ZnO are shown in Fig. 1. The lower curve shows the background absorbance of an evacuated sample, with features at 3700-3400 cm^{-1} and 1600-1300 cm^{-1} due to residual OH^- and $CO_3^=$ species, respectively. The spectra obtained with 75 torr of either H_2 or D_2 are shown superposed in the upper curve. Where changes from the background spectrum are observed, the solid line shows the features caused by H_2 adsorption and the dashed line shows features caused by D_2 adsorption. At full coverage, adsorbed H_2 produces peaks at $\omega_{OH} = 3481$ cm^{-1} and $\omega_{ZnH} = 1712$ cm^{-1}, while adsorbed D_2 produces isotopically shifted peaks at $\omega_{OD} = 2579$ cm^{-1} and $\omega_{ZnD} = 1232$ cm^{-1}.

The specific absorbance for each species, A_i, is evaluated from the intensity vs. coverage measurements. The intensities for OH and ZnH were shown in our previous paper, and are described by the algebraic expressions:

$$N_{OH} = 0.33\ I_{OH} + 0.10\ I_{OH}^2 \qquad (2\text{-}a)$$

$$N_{ZnH} = 0.17\ I_{ZnH} + 0.05\ I_{ZnH}^2 \qquad (2\text{-}b)$$

where N_i is the amount of each species present on the sample (μmole) and I_i is the integrated intensity (cm^{-1}). The corresponding expressions for OD and ZnD determined in this work are:

$$N_{OD} = 0.83 \ I_{OD} + 0.07 \ I_{OD}^{2} \qquad\qquad (2\text{-}c)$$

$$N_{ZnD} = 0.53 \ I_{ZnD} + 0.14 \ I_{ZnD}^{2} \qquad\qquad (2\text{-}d)$$

The specific absorbance, A_i (cm/mole), is then given by (13):

$$A_i = 2.303 \times 10^{6} \ a \ I_i / N_i \qquad\qquad (3)$$

where a is the cross-sectional area of the sample disk (0.97 cm^2). The

zero-coverage limit of A_i is obtained by combining the linear portions of Eqs.

(2-a to 2-d) with Eq. (3). The dipole derivative, $(\partial\mu/\partial r)_i$, which is necessary

for the frequency shift calculations described below, is given by (13):

$$(\partial\mu/\partial r)_i^{2} = (3c^{2}m_r/N_{AV}\pi)A_i \qquad\qquad (4)$$

where c is the speed of light, m_r is the reduced mass of the oscillator, and

N_{AV} is Avogadro's number. The values of $(\partial\mu/\partial r)_i$ obtained in this way are listed

in Table 1 (see below). We note that the value for OH (1.27 D/Å) is comparable

to that reported by Brown for CH_3OH in CCl_4 (1.47 D/Å) (14); no comparison is

available for ZnH.

The coverage dependence of the IR stretching frequencies observed in the

pure component experiments is shown in Fig. 2. The results for H_2 adsorption are

taken from our previous work (5), while the results for D_2 were obtained with

a new sample having a slightly higher surface area. We see that ω_{OH} and ω_{OD}

decrease as adsorbate concentration increases. The total shifts are -17 cm^{-1}

for ω_{OH} and -10 cm^{-1} for ω_{OD}. In contrast, ω_{ZnH} and ω_{ZnD} increase as coverage

increases. The total shifts are also smaller, being 5 cm^{-1} for ω_{ZnH} and 3.5 cm^{-1}

for ω_{OD}. These results are consistent with the work of previous authors

(3, 4, 8).

In Fig. 3, we show the frequency shifts observed in the mixed-isotope

experiments as a function of gas-phase composition. The total pressure in the

cell was kept constant, and the H:D ratio of the gas phase was varied. The

total pressure was high enough that the Type I sites were always saturated.

Thus, the total adsorbate concentration is constant, and only the isotopic

composition of the adsorbate layer is changing. In this work we are primarily concerned with the maximum frequency shifts observed at the two composition extremes, and show the shifts at intermediate composition for completeness. Therefore we retain gas-phase composition as the independent variable in Fig. 3, although we did observe evidence for a slight enrichment of OD and ZnD in the adsorbed phase, relative to the gas phase H:D ratio.

From Fig. 3 we see that ω_{OH} and ω_{OD} are essentially independent of isotopic composition. For example, $\omega_{OH} = 3486$ cm^{-1}, regardless of whether it is surrounded by OH or OD neighbors. This shows that the coverage-induced frequency shifts of ω_{OH} and ω_{OD} are caused by static interactions with neighboring adsorbates. The shifts in ω_{OH} and ω_{OD} cannot be due to dynamic interactions, because dynamic effects, which are strongest between isotopically identical species and which should be negligible between H- and D- oscillators, would produce an isotope effect in the frequency shifts; no such effect is seen in ω_{OH} and ω_{OD}.

In contrast, there is an isotope effect in the ZnD and ZnH frequency shifts: ω_{ZnD} increases as the concentration of D-species in the adsorbate layer increases, and ω_{ZnH} increases as the concentration of H-species increases. In fact, the overall frequency shift and the linear behavior with respect to composition are nearly the same as those observed in the pure component experiments, and appear to be unaffected by the presence of the complementary isotope. This shows that the ZnD and ZnH frequency shifts are due primarily to dynamic interactions, and that purely static effects cancel each other or are absent between Zn-H species.

-5-

IV. Discussion

Coverage-induced frequency shifts in vibrational spectra of adsorbates
can be induced by either dynamic or static interactions between molecules.
These two types of shift can be distinguished experimentally, since dynamic
shifts depend only on the concentration of isotopically similar neighbors,
while static shifts are independent of the isotopic composition of surround-
ing neighbors (7).

Dynamic shifts are generally attributed to electrodynamic interactions
between oscillating dipoles. The theoretical model which describes dynamic
frequency shifts was developed by Hammaker (10), and has subsequently been
discussed by several authors (15-19). All of these discussions have involved
adsorbates on metal surfaces, so that the prediction of frequency shifts
required certain assumptions regarding the effects of image dipoles. The
present work allows a much more straightforward application of dynamic
coupling theory.

In contrast, static shifts may be caused by either electrostatic or
chemical interactions, or both. In order to identify the magnitude of the
chemically-induced shift, which is the quantity of greater interest to the
catalytic chemist, it is first necessary to identify the electrostatic
component of the observed shift. To estimate this quantity, we have modified Bucking-
ham's (11) treatment of solvent-induced frequency shifts to describe the effect
of the electric field due to a neighboring dipole.

In what follows, we shall first discuss the most probable adsorption
site geometry. We then consider the dynamic and electrostatic frequency shifts.
For both types of interaction, we will calculate the shifts predicted for
two occupied nearest neighbor pair sites and then multiply these quantities
by the surface Madelung constant (vide infra) to obtain the total predicted
shifts, for comparison with the observed shifts. The difference between the

observed static shift and the predicted electrostatic shift then represents

the chemically induced shift. We will conclude by offering a qualitative

explanation for the latter quantity, based on inductive interactions

between adsorbates.

Adsorption site geometry. To perform the frequency shift calculations, it is

necessary to specify the geometry of neighboring adsorbates. Boccuzzi et al.

(9) have suggested that Type I H_2 adsorption occurs on a polar ZnO ($000\overline{1}$)

surface. The outermost layer of this surface consists of a hexagonal array

of oxide ions, with one fourth of the ions removed in order to eliminate

the intrinsic surface dipole layer that would be present on an ideally

terminated surface. One argument presented by those authors in support of

the ZnO ($000\overline{1}$) surface is that each missing O anion exposes a cluster of

three adjacent Zn cations. Experimental evidence for such clusters of Zn cations is

given by CO:H_2 co-adsorption studies, which indicate that the Zn cation in a

Type I adsorption site has two neighboring exposed Zn cations (9, 26).

Alternatively, we note that a reconstructed ZnO (0001) surface, which

consists of an hexagonal array of Zn cations with one fourth of the cations missing,

can also provide clusters of adjacent, exposed Zn cations (c.f. Fig. 4).

We believe there are two pieces of experimental evidence which favor the ZnO (0001)

surface. First, the OH stretching region of the ZnO background spectrum is

unchanged by H_2 adsorption. This suggests that there are no surface OH groups

in the areas where H_2 adsorption occurs. It is reasonable to expect that the

Zn-rich ZnO (0001) surface may terminate with bare Zn cations, any

initially present OH groups being driven off as water during the 400 $^\circ$C

pre-treatment. In contrast, one would expect at least part of the O-rich ZnO

($000\overline{1}$) surface to be terminated by OH groups. Thus, we can also

conclude that the observed background OH species are due to ZnO crystal faces on

which H_2 does not adsorb.

The second piece of evidence is that the ZnH species show a dynamic frequency shift, while the OH species do not. As discussed below, this suggests that the ZnH species are parallel and vibrate normal to the surface, while OH species are randomly aligned and/or partially screened from each other as a result of being located in a sub-surface layer. Such ZnH and OH orientations are more likely to be found on the ZnO (0001) surface than on the ZnO (000$\overline{1}$) surface.

In Fig. 4 we show a model of the (2x2) reconstructed ZnO (0001) surface in which one quarter of the Zn cations have been removed. Possible H_2 adsorption sites have been indicated, subject to the constraint that no more than one adorption site exists for each missing Zn cation. With this constraint, we note that the average nearest neighbor separation between Type I sites will be 6.5 Å. Also, we have drawn the figure showing the absorbed H species located directly above the Zn or O ions. It is possible that the H atoms are laterally displaced somewhat, perhaps closer to the three-fold co-ordinated "hollow" sites between ions.

Dynamic Dipole Interactions.   In the presence of an isotopically equivalent neighbor, the frequency (expressed as wave number, cm^{-1}) of a reference dipole is shifted upward from its isolated species value, ω_o, due to coupling with the oscillating electric field produced by a neighboring dipole. The new frequency, ω_{ii}^d, is given by (10, 15):

$$\left[\omega_{ii}^d\right]^2 = \left[\omega_o\right]^2 + \frac{1}{4\pi^2 c^2}\left(\frac{\partial\mu}{\partial r}\right)_i^2 \frac{1}{m_r}\ \phi_{ii} \qquad (5)$$

where ϕ_{ii} is a geometric factor which accounts for the separation and relative orientation of the dipoles:

$$\phi_{ii} = -\ \frac{(\vec{E}_{ii}\cdot\vec{u}_i)}{|\vec{u}_i|^2} \qquad (6)$$

Here $\vec{E}_{ii}$ is the electric field induced by the neighboring dipole at the position of the reference oscillator, and $\vec{\mu}_i$ is the static dipole moment vector of the reference oscillator. Equation (6) is based on the point dipole approximation and the assumption that the static and dynamic dipoles have the same direction. For parallel nearest neighbors $\phi_{ii} = 1/R_{ii}^3$, where R_{ii} is the dipole separation distance.

In Table 1 we list the predicted dynamic shift for each species for a pair of isotopically similar adsorbates separated by 6.5 Å, the average nearest neighbor separation suggested above. The first two columns contain the parameter values for $(\partial\mu/\partial r)$ and ω_o used in the calculation. The dynamic shifts predicted by Eq. (5) are given in the third column. Qualitative agreement with experimental results is already apparent, in that the predicted shifts per dipole pair are much greater for ZnH (0.58 cm^{-1}) and ZnD (0.25 cm^{-1}) than for OH (0.14 cm^{-1}) and OD (0.08 cm^{-1}).

The dynamic shifts calculated above for a single pair of interacting adsorbates cannot be compared directly with the observed dynamic shifts, because the latter reflect interactions with all neighbors. For adsorbed dipoles oriented normal to the surface, the ratio of the total shift to the single nearest neighbor shift is given by the Madelung constant for the surface dipole lattice sum:

$$M = L^3 \sum_{i'} (1/R_{ii'})^3 , \qquad (7)$$

where L is the nearest neighbor separation and the summation is made over all neighbors $R_{ii'}$. If we assume as an upper limit that every Zn vacancy in the reconstructed ZnO (0001) surface creates one H_2 adsorption site, then the adsorption site lattice has hexagonal symmetry, and we can use M = 11.034 (27) to obtain the total predicted shift. These total predicted shifts are

listed in the fourth column of Table 1. For comparison, the observed

shifts are listed in the final column. The latter quantities are the frequency

shifts observed between the composition extremes shown in Fig. 3. Recall

that the results in Fig. 3 were obtained at constant total coverage, so that no changes

in static interactions should be present.

We see that the agreement is quite acceptable for all species

except OH, for which the predicted shift exceeds the observed shift by 0.6 cm^{-1}.

We believe this indicates the OH (and OD) species are not parallel, but instead

are tilted away from the surface normal. The latter orientation would result in a

value of $\phi_{ii} < 1/R_{ii}^{3}$, which would reduce the predicted dynamic frequency shift.

A tilted OH axis would be expected from a valence bond description of H_2

adsorption on the ZnO (0001) surface.

Static dipole interactions. The effect of changes in local environment

on the vibrational frequency of an anharmonic ocsillator has been treated by

Buckingham, who obtained the following expression for solvent induced

static frequency shifts, $\Delta\omega_{ij}^{s}$ (11, 12):

$$\Delta\omega_{ij}^{s} = \left(\frac{B_e}{hc\omega^0}\right)_i \left[\left(\frac{\partial^2 U_{ij}}{\varepsilon_i^2}\right) - 3a\left(\frac{\partial U_{ij}}{\varepsilon_i}\right)\right] \tag{8}$$

where $B_e = [h/(8\pi^2 m_r c r_e^2)]$ is the rotational constant, $\varepsilon = [(r-r_e)/r_e]$ is the

vibrational coordinate, r is the bond length of the reference oscillator,

$a = -(\omega_e x_e / B_e)^{\frac{1}{2}}$ is the first anharmonicity constant of the potential energy

surface of the reference oscillator (28), and U_{ij} is the interaction energy between

the reference oscillator and the surrounding molecules.

As above, we shall apply Eq. (8) to the case of a reference oscillator

interacting with a single neighboring pair site. The electrostatic

contribution to the interaction energy is:

$$U_{ij} = -\vec{E}_{ij} \cdot \vec{\mu}_i \tag{9}$$

Within the point dipole approximation, $\vec{E}_{ij}$ is independent of the reference oscillator vibrational coordinate, and the necessary derivatives for use in Eq. (8) can be obtained using a Taylor series expansion for $\vec{\mu}_i$:

$$\vec{\mu}_i = \vec{e} \, [\mu + (\partial\mu/\partial r)\Delta r + \ldots] \tag{10}$$

where $\vec{e}$ is the unit vector parallel to the adsorbate bond axis and μ is the dipole moment, including sign. We can make no estimate of the second order and the higher dipole derivatives for these adsorbates, but expect them to be small relative to the first derivative (22). For example, the absence of significant intensity in the $0 \rightarrow 2$ overtone of the ZnH mode implies a small anharmonicity, and hence very small values for the higher order dipole derivatives.

Combining Eqs. (8-10), we obtain our final expression for the electrostatic frequency shift, $\Delta\omega_{ij}{}^{es}$:

$$\Delta\omega_{ij}{}^{es} = \left(\frac{3B_e r_e a}{hc\omega_o}\right)_i (\frac{\partial\mu}{\partial r})_i \, (\vec{E}_{ij} \cdot \vec{e}_i) \tag{11}$$

Because the relative frequency shift, $\Delta\omega^{es}/\omega_o$, is nearly independent of isotropic identity for static interactions, we will only examine the electrostatic frequency shifts for ω_{ZnH} and ω_{OH}. The additional parameters needed for this calculation are $r_e = 1.595$ Å and $a = -2.88$ for ZnH, $r_e = 0.970$ Å and $a = -2.12$ for OH (23). The static dipole moment is estimated to be $\mu = -0.47$ D for ZnH (1 Debye $= 10^{-18}$ esu-cm), based on the percentage of ionic character predicted by the Pauling electronegativity difference (24), and $\mu = 1.59$ D for OH, based on the observed dipole moment of H_2O (25). The absolute values of $(\partial\mu/\partial r)$ were given in Table 1, and the signs are assumed to be the same as for μ.

The frequency shifts predicted by Eq. (11) for each of the four pairings of reference and neighboring dipoles are listed in Table II. For simplicity, we have again assumed parallel dipoles and 6.5 Å for the nearest neighbor separation, recognizing that the former assumption will overestimate the electrostatic shift for OH species. The predicted total shift for each reference

-11-

species, i, is obtained by adding the two shifts due to both types of neighbor species, j, and multiplying by the Madelung constant (=11.034). We do not include the shift due to interactions between the ZnH and OH dipoles that occupy the reference pair site; since these two species are always present simultaneously (cf. Eq. 1), their "self-interaction" cannot be resolved experimentally. The predicted electrostatic shifts can be compared with the observed static shifts, given in the fourth column of Table II. The latter are obtained from the total shifts observed in Fig. 2 by subtracting the dynamic shifts found in Fig. 3

We note that the predicted electrostatic shift is positive for OH and negative for ZnH. This can be explained physically as follows: The net dipole moment at an occupied H_2 site is positive (i.e., $\mu_{OH} + \mu_{ZnH} > 0$). Therefore, an occupied neighboring site produces a negative electric field at the reference site. This produces a decrease in the equilibrium OH bond length and an increase in the ZnH bond length, since $(\partial \mu / \partial r)_{OH} > 0$ and $(\partial \mu / \partial r)_{ZnH} < 0$ (c.f. Eq. 9). Since the anharmonicity constant is negative, the new equilibrium bond lengths produce a positive frequency shift in ω_{OH} and a negative shift in ω_{ZnH}.

Chemical (inductive) interactions. The difference between the observed static shift and the calculated electrostatic contribution is listed in the final column of Table II for each reference species. These differences are attributed to chemical interactions between adsorbates. The chemical shift is -26 cm^{-1} for ω_{OH} and +22 cm^{-1} for ω_{ZnH}.

Boccuzzi et al. (8) have attributed the observed negative OH frequency shift to a decrease in OH bond polarity, caused by a depolarization of the ZnO surface brought about by H_2 adsorption. While this would appear to be a reasonable explanation for the OH shift alone, we note that H_2 induced polarization should also decrease the ZnH bond polarity and produce a negative ZnH shift. However, the results in Table II indicate that a positive chemical

-12-

shift exists for ZnH, which suggests an increase in polarity for the ZnH bond.

Instead, we offer the following alternative explanation for chemically—
induced frequency shifts based on arguments analogous to those for inductive
effects observed in vibrational spectra of organic molecules (30).
As suggested schmatically by Eq. (1), a vacant site capable of homolytic
H_2 dissociation must be able to provide two electrons in order to complete
both new adsorbate bonds. Thus, we can consider H_2 adsorption to be an
electron localizing process with regard to electron density initially present
at a vacant site. H_2 adsorption will decrease the available electron
density at neighboring sites (i.e., a negative σ-induction effect (30)). This
will decrease the polarity of the OH bond, in which O is the electronegative
partner, and increase the polarity of the ZnH bond, in which Zn is the electro-
positive partner. Therefore, the effect of neighboring H_2 adsorbates will be to
produce a negative inductive contribution to the OH frequency shift and a
positive contribution to the ZnH shift. From the results in Table II, we can
conclude that for OH species the chemical contribution outweighs the electro-
static, and a net negative static shift is observed. For ZnH, the chemical
and electrostatic shifts fortuitously cancel, so that no net static shift is
seen.

We emphasize that the proposed electron localization model offers a simple
description of the chemically induced contribution to the OH and ZnH static
frequency shifts. The inductive interaction provides an equally staightforward
explanation for H_2-CO frequency interactions in that co-adsorption system, as
we will describe in a subsequent publication (26).

V. Summary

Using pure- and mixed-isotope studies of H_2 adsorption of ZnO, we have
shown that the coverage-induced shifts of ZnH and ZnD are dynamic in origin,
while the shifts of OH and OD are due to static interactions. The dynamic

-13-

ω_{ZnH} and ω_{ZnD} shifts are described well by Hammaker's treatment of dynamic dipole interactions; a comparison of the predicted shift for a pair of nearest neighbor adsorbates with the observed total shift yields a value for the surface dipole Madelung sum which is consistent with an adsorption geometry based on a reconstructed polar ZnO surface, assuming an average site separation distance of 6.5 Å. Dynamic ω_{OH} and ω_{OD} shifts are completely absent. Also the absence of background OH shifts suggests that adsorption occurs on ZnO (0001) surfaces that are free of residual OH groups.

The observed static OH shift and the negligible static ZnH shift appear to be the result of completing electrostatic and inductive interactions. For OH, electrostatic interactions produce a positive contribution while chemical interactions make a larger, negative contribution. For ZnH, electrostatic interactions produce a negative contribution while chemical interactions produce an equal, positive contribution. The electrostatic shifts can be predicted using a modification of Buckingham's treatment of solvent-induced shifts to describe the effect of electric fields due to neighboring dipoles. The inductive shifts can be qualitatively described by considering H_2 adsorption to be an electron-localizing process which causes neighboring OH bond polarities to decrease and the ZnH bond polarities to increase as H_2 coverage increases.

VI. Acknowledgements

References

1. P.J. Denny and D. A. Whan, in _Catalysis, Vol. 2_, Specialist Periodic Reports (D.A. Dowden and C. Kemball, eds.) (The Chemical Society, London, 1977) p. 79.

2. R. G. Hermann, K. Klier, G. W. Simmons, B. P. Finn, and J. B. Bulko, J. Catal. 56, 407 (1979).

3. R. P. Eishchens, W. A. Pliskin, and M. J. D. Low, J. Catal. 1 180 (1962).

4. R. J. Kokes, A. L. Dent, C. C. Chang, and L. T. Dixon, JACS 94 4429 (1972).

5. G. L. Griffin and J. T. Yates, Jr. (submitted for publication, J. Catalysis).

6. _Vibrational Spectroscopies for Adsorbed Species_ (A. T. Bell and M. L. Hair, eds.) ACS (New York) 1980.

7. P. Hollins and J. Pritchard, Surf. Sci 89 486 (1979).

8. F. Boccuzzi, E. Barello, A. Zecchina, A. Bossi, and M. Camia, J. Catal. 51 150 (1978).

9. F. Boccuzzi, E. Garrone, A. Zecchina, A. Bossi, and M. Camia, J. Catal. 51 160 (1978).

10. R. M. Hammaker, S. A. Francis, and R. P. Eischens, Spectrochimica Acta 21 1295 (1965).

11. A. D. Buckingham, Proc. Roy. Soc. Lon., Ser. A 248 169 (1958).

12. A. D. Buckingham, Trans. Faraday Soc. 56 753 (1960).

13. D. A. Seanor and C. H. Amberg, J. Chem. Phys. 42 2967 (1965).

14. T. L. Brown and M. T. Rogers, JACS, 79 577 (1957).

15. A. Crossley and D. A. King, Surf. Sci. 68 528 (1977).

16. M. Moskovits and J. E. Hulse, Surf. Sci. 78 397 (1978).

17. M. Scheffler, Surf. Sci. 81 562 (1979).

18. S. Efrima and H. Metiu, Surf. Sci. 92 433 (1980).

19. H. Pfnur, D. Menzel, F. M. Hoffmann, A. Ortega, and A. M. Bradshaw, Surf. Sci. 93 431 (1980).

20. S. C. Abrahams and J. L. Bernstein, Acta Crystal. B25 1233 (1963).

21. A. L. Dent and R. J. Kokes, J. Phys. Chem. 73 3772 (1969).

22. R. A. Toth, R. H. Hunt, and E. K. Plyler, J. Molecular Spectroscopy
    <u>32</u> 85 (1969).

23. G. Herzberg, <u>Spectra of Diatromic Molecules</u> (Van Nostrand, Princeton,
    NJ, 1950).

24. L. Pauling, <u>The Chemical Bond</u> (Cornell University Press, Ithaca, 1967),
    p. 64.

25. R. D. Nelson, Fr., D. R. Lide, Fr., and A. A. Maryott "Selected Values of
    Dipole Moments for Molecules in the Gas Phase" National Reference
    Data Service, NSRDS-NBS 10.

26. G. L. Griffin and J. T. Yates, Jr. (To be submitted).

27. B. R. A. Nijboer and F. W. de Wette; Physica <u>24</u> 422 (1958).

28. The relationship between the spectroscopic anharmonicity, $\omega_e x_e$, and
    the higher-order terms in the potential energy function of the oscil-
    lator is $\omega_e x_e = (3Be/2)\ (b-(5/4)a^2)$, where a and b are coefficients
    in the series expansion for the potential (11): $V(\xi) = (hc\omega_e^2/4Be)\xi^2$
    $[1 + a + b\ ^2 + ...]$. For an arbitrary potential, a and b cannot be
    determined from knowledge of $\omega_e x_e$ alone. If a Morse potential is
    assumed, then $a^2/b = 7/12$ (29) and we obtain $a = -(\omega_e x_e/Be)^{\frac{1}{2}}$. The
    role of the Morse potential for relating a to $\omega_e x_e$ apparently has
    not been explicitly noted by other authors using Buckingham's results.

29. M. Karplus and R. N. Porter; <u>Atoms and Molecules</u> (W. A. Benjamin, Inc.,
    Menlo Park, 1971) p. 476.

30. L. S. Bellamy "Infrared Group Frequencies," (Methuen, London, 1968)
    p. 390 ff.

Figure Captions

1. IR survey spectra of reversible adsorption of H_2 and D_2 on ZnO at 300 K. Lower spectrum: ZnO background (evacuated). Upper spectra: — P_{H_2} = 75 torr; --- P_{D_2} = 75 torr.

2. Coverage dependence of IR stretching frequencies for pure H_2 or D_2 adsorbed on ZnO.

3. Coverage dependence of IR stretching frequencies for H_2-D_2 mixtures adsorbed on ZnO. T = 300 K, P_{H_2} + P_{D_2} = 87.5 torr.

4. Diagram of (2 x 2) reconstructed ZnO (0001) surface showing possible H_2 adsorption sites.

Table 1: Calculated IR frequency shifts based on dynamic dipole interactions: Comparison with observed shifts for isotopic dilution at constant total coverage.

Adsorbate Species	$\|\partial\mu/\partial r\|$ (D/Å)[a]	ω_0 (cm^{-1})	$(\Delta\omega_{ii}^d)$[b] (cm^{-1})	Total shift (cm^{-1}) predicted[c]	observed[d]
OH	1.27	3498	0.14	1.6	< 1.0
OD	1.13	2589	0.076	0.8	< 1.0
ZnH	1.79	1707	0.58	6.4	5.0
ZnD	1.42	1228	0.25	2.8	3.5

a) 1 D/Å $= 10^{-10}$ esu

b) Single neighbor interaction, $R_{ii} = 6.5$ Å

c) Given by $11.034 \cdot (\Delta\omega_{ii}^d)$

d) From Fig. 3

Table II: Calculated electrostatic contribution to IR frequency shifts: comparison with observed pure component frequency shifts, corrected for dynamic contributions.

Reference species (i)	Neighboring species (j)	$\Delta\omega_{ij}^{es}$ [a] (cm^{-1})	Total shift (cm^{-1}) electrostatic [b]	observed [c]	inductive [d]
OH	OH	1.2			
	ZnH	-0.4			
	Σ (=$\Delta\omega_i^{es}$)	0.8	9.0	-17.0 ± 1.5	-26
ZnH	ZnH	0.8			
	OH	-2.7			
	Σ (=$\Delta\omega_i^{es}$)	-2.0	-22.1	-0.0 ± 1.5	+22

[a] Single neighbor interaction, $R_{ij} = 6.5$ Å

[b] Given by $(11.034)(\Delta\omega_i^{es})$

[c] Will include electrostatic and chemical interactions

[d] Difference between observed shift and calculated electrostatic contribution

IR Spectra of Reversible Adsorption of H₂ and D₂ on ZnO (T = 300 K)
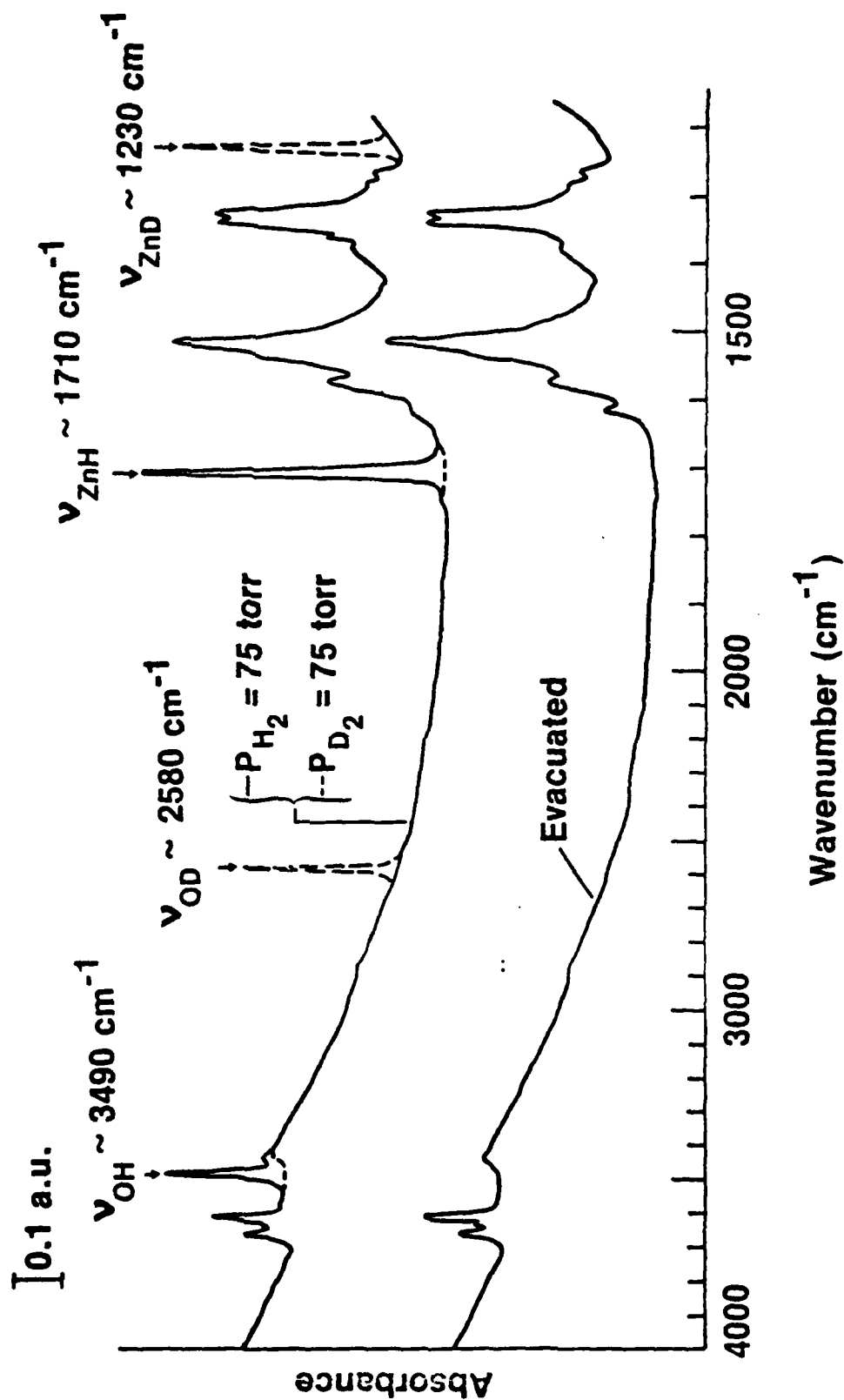
Figure 1

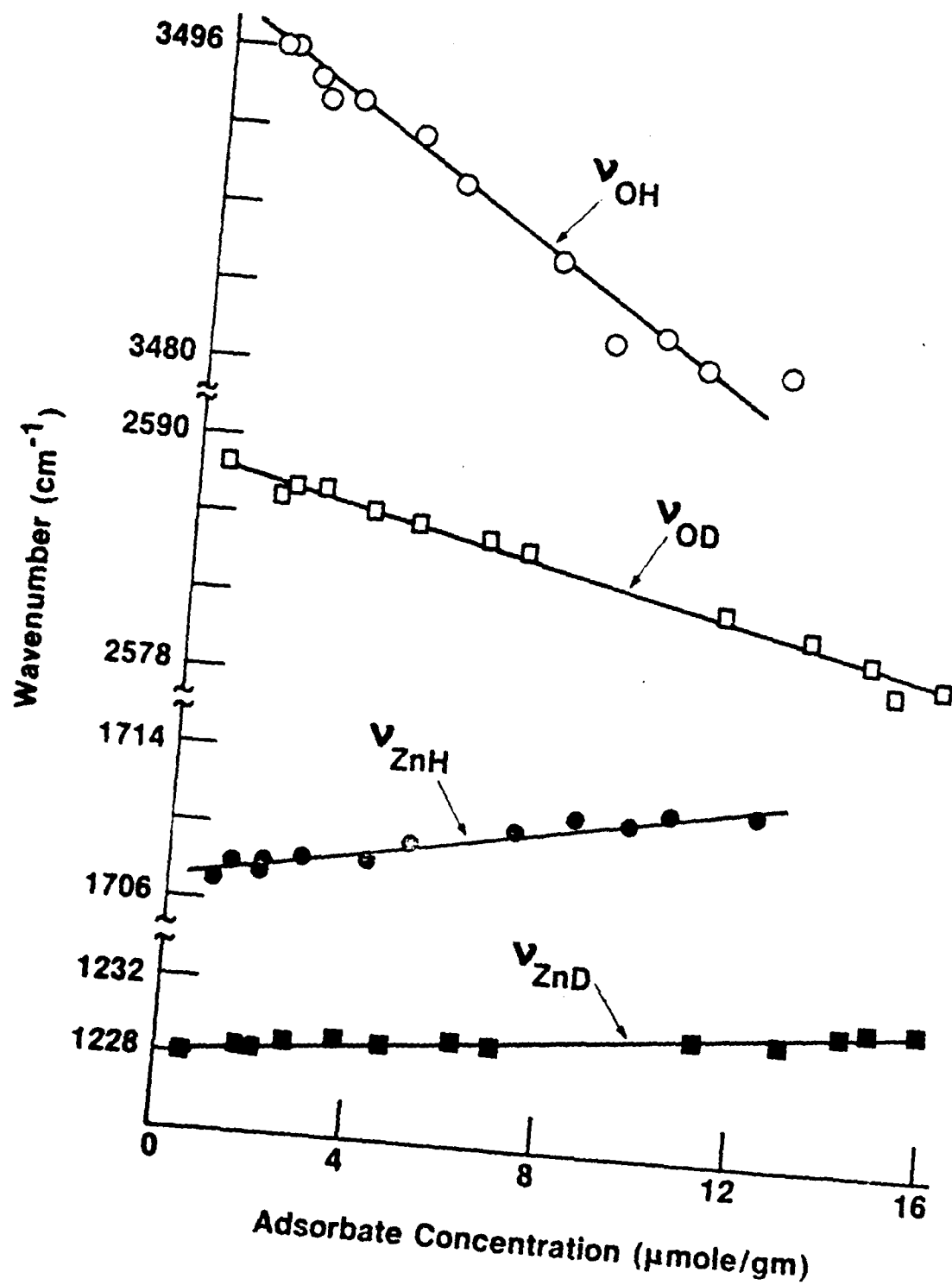Coverage Dependence of IR Stretching Frequencies for Pure H_2 (D_2) Adsorbed on ZnO

Figure 2

Coverage Dependence of IR Stretching Frequencies for H_2-D_2 Mixtures Adsorbed On ZnO (300 K, P_{TOT} = 87.5 torr)

ν_{OH}

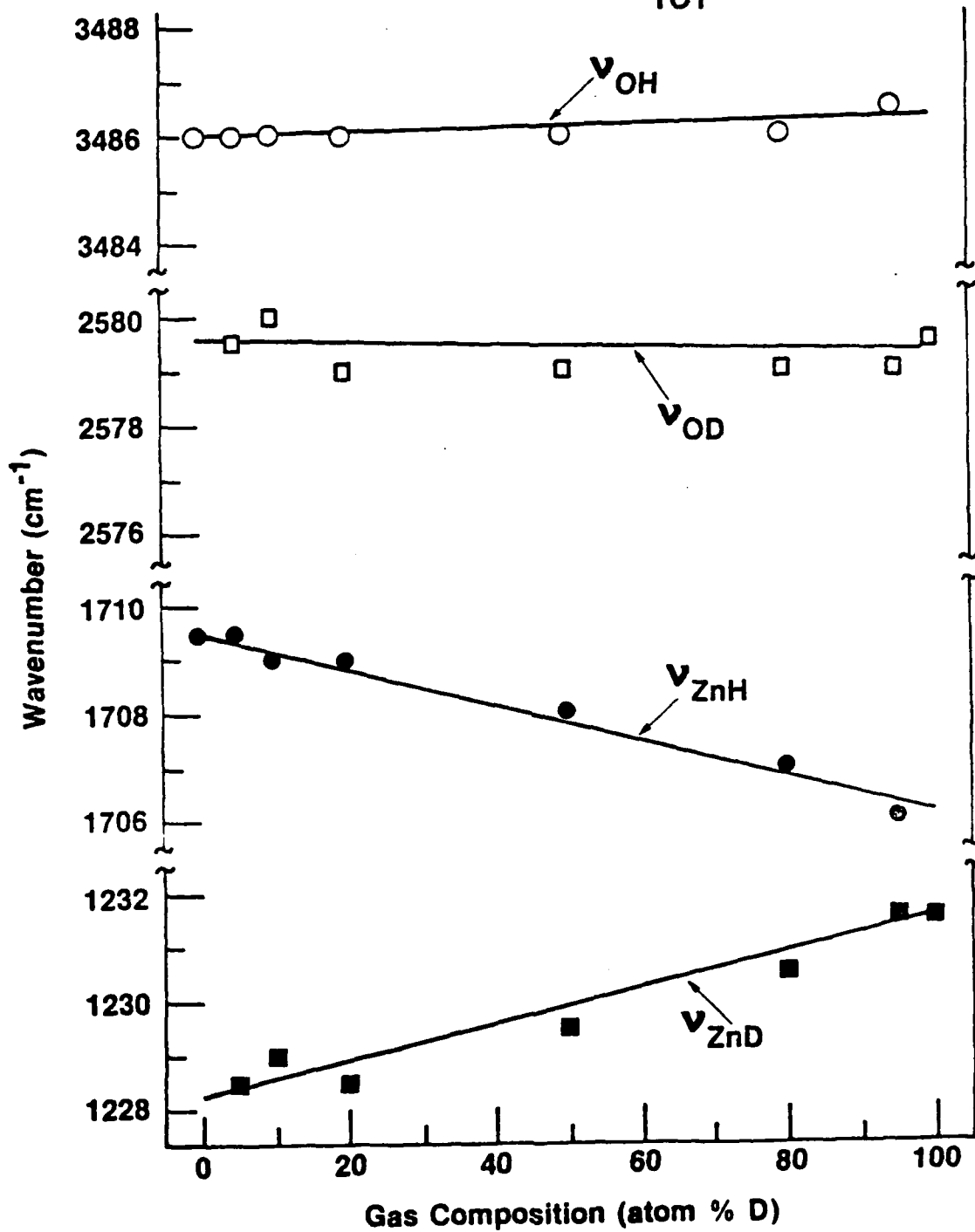ν_{OD}

ν_{ZnH}

ν_{ZnD}

Wavenumber (cm^{-1})

Gas Composition (atom % D)

Figure 3

Possible Type I H_2 Adsorption Pair Site Geometry on (2x2) Reconstructed ZnO (0001)

3.25 Å

= $O^=$

= Zn^{++}

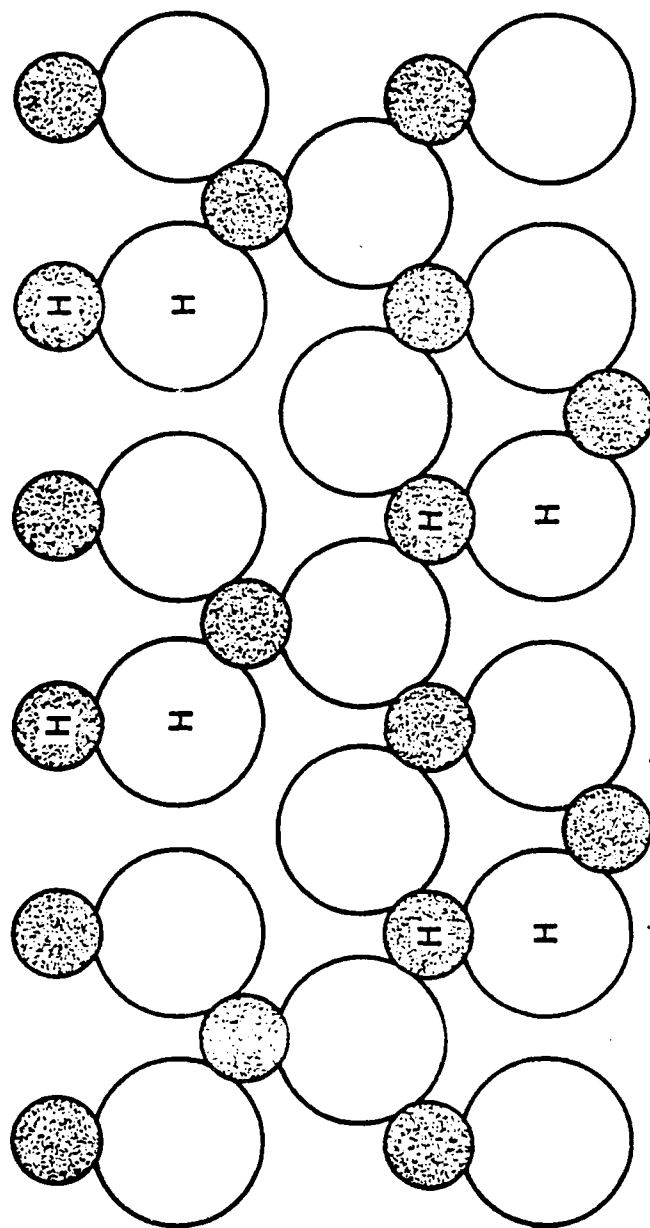Figure 4

SECURITY CLASSIFICATION OF THIS PAGE (When Data Entered)

REPORT DOCUMENTATION PAGE	READ INSTRUCTIONS BEFORE COMPLETING FORM

1. REPORT NUMBER	2. GOVT ACCESSION NO.	3. RECIPIENT'S CATALOG NUMBER
Technical Report #25	AD-A	

4. TITLE (and Subtitle)	5. TYPE OF REPORT & PERIOD
Adsorption of H_2 Isotopes on ZnO: Coverage Induced IR Frequency Shifts and Adsorbate Geometry	
	6. PERFORMING ORG. REPORT NUMBER

7. AUTHOR(s)	8. CONTRACT OR GRANT NUMBER
Gregory L. Griffin John T. Yates, Jr.	N0014-81-F-0008 Mod. No. P00001

9. PERFORMING ORGANIZATION NAME AND ADDRESS	10. PROGRAM ELEMENT PROJECT AREA & WORK UNIT NUMBERS
Surface Science Division National Bureau of Standards Washington, DC 20234	

11. CONTROLLING OFFICE NAME AND ADDRESS	12. REPORT DATE
	February 1, 1982
	13. NUMBER OF PAGES

14. MONITORING AGENCY NAME & ADDRESS(if different from Controlling Office)	15. SECURITY CLASS (of this report)
	Unclassified
	15a. DECLASSIFICATION DOWNGRADING SCHEDULE

16. DISTRIBUTION STATEMENT (of this Report)

Approved for Public Release; Distribution Unlimited

17. DISTRIBUTION STATEMENT (of the abstract entered in Block 20, if different from Report)

18. SUPPLEMENTARY NOTES

To be published in J. Chem. Physics

19. KEY WORDS (Continue on reverse side if necessary and identify by block number)

Chemisorption; hydrogen; IR frequency studies; zinc oxide.

20. ABSTRACT (Continue on reverse side if necessary and identify by block number)

The coverage dependence of the IR stretching frequencies for dissociative Type I adsorption of H_2 and D_2 on ZnO powders has been measured using transmission IR spectroscopy. By comparing the frequency shifts observed when the isotopic composition of the adsorbate is varied at constant total coverage with the shifts observed when the total coverage of either pure component is varied, we can separate the dynamic and static contributions to the coverage .

(continued on reverse side)

DD FORM 1473 , 1 JAN 73   EDITION OF 1 NOV 65 IS OBSOLETE
S N 0102-014-6601

Item 20. Continued

induced frequency shifts. The ZnH and ZnD shifts are due primarily to electro-
dynamic interactions. The observed shifts are in good agreement with the Hammaker
model for dynamic dipole-dipole interactions, if adsorption is assumed to occur
on (2x2) reconstructed ZnO (0001) surface planes. In contrast, the OH and OD
shifts are due to electrostatic and inductive interactions. The electrostatic
contribution can be estimated using a modification of Buckingham's treatment
of local environment effects. A qualitative model, based on electron locali-
zation effects is presented to explain the observed inductive contribution.